RESEARCH PAPER

Evaluation of In-vivo Bioavailability Potential of Tenofovir loaded Solid Lipid Nanoparticles

Seetha Devi Alla[1], Meraj Sulthana Syed[2], Sri Rekha Malakapurapu[3*], Chundu Sai Navya Sri[4], Gullapalli Mugibunnisa[5], Kathi Nagendram[6] and Darla Pavithra[7]

[1]Professor, Dept. of Pharmaceutics, Gokaraju Rangaraju College of Pharmacy, Bachupally, Hyderabad, Telengana, India-500090
[2]Assistant Professor, Dept. of Pharmaceutics, Chebrolu Hanumaiah Institute of Pharmaceutical Sciences, Chowdavaram, Guntur-522019, Andhra Pradesh, India
[3]Assistant Professor, Dept. of Pharmaceutics, Hindu College of Pharmacy, Amaravathi Road, Guntur, Andhra Pradesh, India-522002*
[4]B Pharm, Dept. of Pharmaceutics, Hindu College of Pharmacy, Amaravathi Road, Guntur, Andhra Pradesh, India-522002
[5]B Pharm, Dept. of Pharmaceutics, Hindu College of Pharmacy, Amaravathi Road, Guntur, Andhra Pradesh, India-522002
[6]B Pharm, Dept. of Pharmaceutics, Hindu College of Pharmacy, Amaravathi Road, Guntur, Andhra Pradesh, India-522002
[7]B Pharm, Dept. of Pharmaceutics, Hindu College of Pharmacy, Amaravathi Road, Guntur, Andhra Pradesh, India-522002
Email Id: [1]Seethagottipati@gmail.com, [2]syedmerajsultana45@gmail.com, [3]rekhashankarsutari@gmail.com, [4]navyachowdary1305@gmail.com, [5]mugibunnisa1996@gmail.com, [6]nagendramkathi909@gmail.com and [7]pavithradarla543@gmail.com
***Corresponding Author:** Dr. Sri Rekha Malakapurapu*
Email ID: rekhashankarsutari@gmail.com

Received: 24th April, 2026; Revised: 20th May 2026; Accepted: 30th June, 2026; Available Online: 10th July, 2026

ABSTRACT

Background: Current study aims to develop orally administered Tenofovir (TNF) loaded Solid Lipid Nanoparticles (SLNs) to enhance systemic absorption and to evaluate its tissue distribution in brain. Tenofovir, an antiviral drug used in HIV therapy, suffers from poor oral bioavailability and limited penetration across the blood–brain barrier (BBB). Since the central nervous system serves as a major HIV reservoir, effective CNS delivery of anti-HIV agents remains a critical therapeutic challenge.

Methods: TNF-loaded SLNs were prepared using the microemulsion technique with Compritol ATO 888 as the lipid. All formulations underwent extensive testing for particle size, polydispersity index (PDI), zeta potential, entrapment efficiency, and in vitro drug release, while the effects of lipid concentration, surfactant concentration, and homogenisation time were optimized. The optimized formulation was further characterized by SEM, DSC, and PXRD, followed by in vivo bioavailability, tissue distribution, and short-term stability studies.

Results: The optimized formulation (F7) containing 5% w/v lipid and 1.5% w/v surfactant exhibited a particle size of 195.4 ± 8.2 nm, PDI of 0.26 ± 0.02, entrapment efficiency of 82.7 ± 2.9%, and sustained drug release of 86.42 ± 3.41% over 24 hrs. Pharmacokinetic studies demonstrated a 7.2-fold enhancement in oral bioavailability and significant brain accumulation (38.12 ± 0.26%) of TNF.

Conclusion: The findings highlight SLNs as a promising oral delivery system for enhancing Tenofovir bioavailability and brain targeting, offering potential for improved management of HIV-associated CNS reservoirs.

Keywords: Tenofovir, Solid Lipid Nanoparticles, Brain delivery, Blood Brain Barrier, Compritol ATO 888, Microemulsion technique.

How to cite this article: Alla SD, Syed MS, Malakapurapu SR, Sri CSN, Gullapalli M, Kathi N, Darla P, Evaluation of In-vivo Bioavailability Potential of Tenofovir loaded Solid Lipid Nanoparticles. Int J Drug Deliv Technol. 2026;16(7):632-645. DOI: 10.25258/ijddt.16.7.66
Source of support: Nil.
Conflict of interest: None

**Author for Correspondence: rekhashankarsutari@gmail.com*

GRAPHICAL ABSTRACT

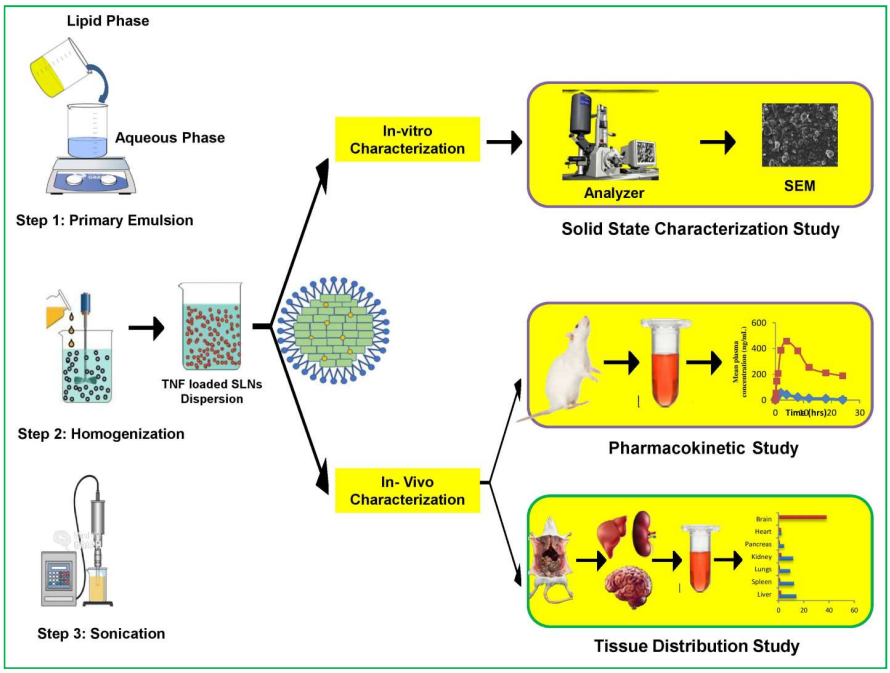

INTRODUCTION

Tenofovir (TNF) is a hydrophilic nucleoside reverse transcriptase inhibitor [1] used for HIV/AIDS [2-4] and chronic hepatitis B [5, 6]. Classified as a BCS class III drug, it exhibits high solubility (5 mg/mL) [7] but poor permeability (log P −1.6) [8], resulting in low and variable oral bioavailability due to limited intestinal absorption, gut metabolism, and P-glycoprotein efflux [9-11]. Prodrugs such as TDF and TAF partially improve permeability but remain susceptible to metabolic degradation, highlighting the need for novel delivery strategies [12-17].

Although HAART regimens [18-20], including tenofovir, effectively reduce plasma viral loads, 75–90% of patients develop neurological complications, [21] reflecting inadequate CNS drug delivery. Poor BBB penetration, due to hydrophilicity [22] and active efflux [23], allows the brain to serve as a viral reservoir, contributing to HIV-associated neurocognitive disorders and encephalitis [24-27].

Nanocarrier systems, particularly solid lipid nanoparticles (SLNs), offer a promising strategy to enhance oral bioavailability and CNS targeting [28-31]. SLNs provide biocompatibility, controlled release, high drug-loading capacity, lymphatic uptake, and protection from enzymatic degradation, while reducing drug efflux [32-38]. Despite these advantages, SLNs for oral Tenofovir delivery remain underexplored.

This study aimed to develop Tenofovir-loaded SLNs using the microemulsion method with Compritol ATO 888 and Poloxamer-188, evaluating physicochemical properties, in vivo pharmacokinetics, and tissue distribution, with the goal of improving oral bioavailability and brain delivery of Tenofovir.

MATERIALS AND METHODS

MATERIALS: MSN Laboratories Pvt. Ltd. (Hyderabad, India) kindly supplied tenofovir and Compritol® 888 ATO. Researchers bought tripalmitin, stearic acid, poloxamer 188, and soy lecithin from Sigma-Aldrich Chemicals Pvt. Ltd. (Bangalore, India). Dialysis membranes (molecular weight cut-off 12,000–14,000 Da) were obtained from HiMedia Laboratories Pvt. Ltd. (Mumbai, India). Nylon syringe filters (0.45 µm pore size, 25 mm diameter) were procured from Labsoul (India). Water, methanol, and acetonitrile of HPLC quality were acquired from Thermo Fisher Scientific India Pvt. Ltd. (Mumbai, India). The Albino Wistar rats were imported by Mahaveera Enterprises in Hyderabad, India. The remaining chemicals and solvents were of analytical quality.

METHODS

Lipid Screening: Lipid screening was performed based on the solubility of Tenofovir in different solid lipids, including tripalmitin, Compritol® ATO 888, glyceryl monostearate, and stearic acid. Briefly, 5 mg of Tenofovir was incrementally added to each molten lipid maintained at 5 °C above its melting point until a clear solution was obtained. The total amount of drug solubilized was recorded, and the lipid exhibiting the highest solubility was selected for formulation development [39].

Surfactant Screening: Surfactants were screened based on their ability to produce SLNs with minimum particle size and maximum entrapment efficiency. Span 60, Tween 80, Poloxamer 188, and Poloxamer 407 were evaluated by

preparing trial SLN batches with the selected lipid. The surfactant that produced the greatest drug entrapment and the lowest particle size was chosen after particle size and entrapment efficiency were compared [40].

Drug-Excipient Compliance: Fourier Transform Infrared (FTIR) spectroscopy was used to evaluate drug-excipient suitability. Spectra of pure Tenofovir, Compritol® ATO 888, Poloxamer 188, and their physical mixture were recorded over a range of 4000–400 cm^{-1} and compared for any significant spectral shifts or disappearance of characteristic peaks [41].

Preparation of Tenofovir-Loaded Solid Lipid Nanoparticles

An improved microemulsion approach was utilized to produce tenofovir-loaded SLNs. [42]. Compritol® ATO 888 was used as the lipid, Poloxamer 188 as the surfactant, and soya lecithin (0.5% w/v) as the co-surfactant. By adjusting the concentration of lipids, surfactants, and homogenization times, twelve formulations were created as tabulated in Table 1. Tenofovir was dissolved in molten lipid maintained at 75 °C. Initially to produce a primary emulsion, the aqueous phase containing surfactant and co-surfactant was heated to the same temperature and added dropwise to the lipid phase while being continuously stirred at 500 rpm. Then this primary emulsion was dispersed into ice-cold water (2–3 °C) under high-speed homogenization, followed by ultrasonication for 10 min to obtain nanosized SLNs.

Table 1: Formulation composition for Tenofovir (TNF) loaded Solid Lipid Nanoparticles

Formulation Code	Concentration of Lipid(%w/v) (Compritol 888 ATO)	Concentration of Surfactant (% w/v) (Poloxamer-188)	Homogenization Time (min)
F1	2.5	1	60
F2	5	1	60
F3	7.5	1	60
F4	10	1	60
F5	5	0.5	60
F6	5	1	60
F7	5	1.5	60
F8	5	2	60
F9	5	1	30
F10	5	1	60
F11	5	1	75
F12	5	1	90

EVALUATION OF TNF- LOADED SOLID LIPID NANOPARTICLES:

Average Particle Diameter and Polydispersity Index: Using a nanoparticle size analyzer (SZ-100Z, Horiba, Japan) by the mechanism of dynamic light scattering, particle diameter and polydispersity index (PDI) were measured. Analyses were performed at a scattering angle of 90° after the formulations were diluted 1:100 with double-distilled water prior to measurement [43].

Zeta Potential: Zeta potential was measured using a Zetasizer Nano ZS (Malvern Instruments, UK) after dilution with double-distilled water, at 25 °C and an applied voltage of 3.3 V [43, 44].

Entrapment Efficiency: Centrifugation was used to calculate the percentage of entrapment at 5000 rpm for 10 min. The unentrapped drug in the supernatant was quantified spectrophotometrically at 260 nm, and %EE was calculated using a standard formula [43, 45].

$$\%\text{Entrapment Efficiency} = \frac{\text{Total drug content} - \text{Unentrapped drug}}{\text{Total drug content}} \times 100$$

In-vitro Drug Release Study: The dialysis bag diffusion method was used to assess the release of Tenofovir-loaded SLNs and pure drug suspension. The study was carried out at 37 ± 0.5°C and 100 rpm in 0.02 M HCl (pH 1.2) for the first two hours, then in phosphate buffer (pH 7.4). Samples equal to 10 mg of Tenofovir were put in the bag and submerged in 100 mL of dissolving medium after dialysis membranes (MWCO 12,000-14,000 Da) had been pre-soaked overnight. To quantify cumulative drug release, aliquots were removed at predefined intervals (0-24 hours), replaced with new media, and spectrophotometrically measured at 260 nm [46,47].

CHARACTERIZATION OF OPTIMIZED FORMULATION:

Differential Scanning Calorimetry (DSC): Thermal behaviour of pure Tenofovir, physical mixture (Tenofovir, Compritol® ATO 888, and Poloxamer 188), and optimized SLNs (F7) was analyzed using DSC. per minute in a nitrogen environment (30 mL per minute) between 30 and 300°C [48].

Powder X-Ray Diffraction (PXRD): Cu Kα radiation (λ = 1.5418 Å) operating at 40 kV and 15 mA was used in powder X-ray diffraction (PXRD) to investigate the crystalline characteristics of the pure drug, physical

mixture, and optimized SLNs. Diffractograms were captured at a scanning speed of 5°/min throughout a 2θ range of 30-90° [49].

Scanning Electron Microscopy (SEM): Surface morphology of optimized TNF-loaded SLNs was evaluated using SEM. Samples were mounted on aluminium stubs, and images were recorded at 15 kV with 1 kX magnification [50].

IN-VIVO PHARMACOKINETIC STUDY:

Study Design and Ethics: The Institutional Animal Ethics Committee at Hindu College of Pharmacy in Guntur, India, approved the use of animals in the research (IAEC-HCOP/2022/07). A week before to the studies, albino Wistar rats weighing 200–300 g of either sex were acclimated to typical laboratory conditions (25 ± 2°C, 60 ± 5% relative humidity, and a 12-hour light/dark cycle), with unlimited access to food and water [51].

Analytical Method: Plasma Tenofovir concentrations were quantified using a validated HPLC method [52]. Acetonitrile: water (75:25, v/v) was used as the mobile phase for chromatography on a Shim-Pack GIST C18 column at a flow rate of 1 mL/min. The detection process was run for ten minutes at a wavelength of 262 nm.

Experimental Procedure: Eighteen rats were randomized into three groups (n=6): Group I received pure Tenofovir solution (10 mg/kg), Group II received optimized TNF-loaded SLNs (equivalent to 10 mg/kg), and Group III received phosphate buffer saline. Dosing was performed orally after overnight fasting. Blood samples were collected at predetermined intervals (0-24 h) via the retro-orbital plexus, centrifuged at 5000 rpm for 15 min, and plasma samples were stored at -20°C until analysis [51, 53].

Plasma Sample Preparation: Plasma proteins were precipitated using 5% perchloric acid (1:1 v/v), followed by vertexing and centrifugation at 10,000 rpm for 10 min at 4°C. The supernatant was filtered (0.45 µm) and directly injected into the HPLC system for analysis [54,55].

Pharmacokinetic Analysis: Pharmacokinetic parameters (Cmax, Tmax, AUC_{0-24}, Ke, t½, and MRT) were calculated using non-compartmental analysis. Relative bioavailability was determined by comparing AUC_{0-24} values of SLNs with pure Tenofovir solution [55,56].

Tissue Distribution Study: After 24 h, animals were sacrificed, and organs (liver, spleen, lungs, pancreas, kidney, heart, and brain) were collected, homogenized in phosphate buffer, and centrifuged at 15,000rpm for 30 min. The supernatant was filtered and analyzed using the validated HPLC method [57,58].

Statistical Analysis: mean ± SD is used to express all data. Student's t-test was used to assess statistical significance between groups; $p < 0.05$ was deemed significant [55,56].

SHORT TERM STABILITY STUDIES: Stability studies of the optimized TNF-loaded SLNs (F7) were conducted for 180 days under three storage conditions: 5±3°C/45% RH, 30±2 °C/65% RH, and 40±2°C/75% RH using a stability chamber. Samples were assessed for variations in entrapment efficiency, zeta potential, and particle size at predefined intervals [59].

RESULTS

Lipid and Surfactant Screening: Lipid screening was conducted using tripalmitin, Compritol® 888 ATO, glyceryl monostearate, and stearic acid based on Tenofovir solubility. As shown in Figure 1, Compritol® 888 ATO exhibited the highest drug solubility and was therefore selected as the lipid phase to achieve higher drug loading. Surfactant screening using Span 60, Tween 80, Poloxamer 188, and Poloxamer 407 demonstrated that formulations containing Poloxamer 188 produced the smallest particle size and highest entrapment efficiency (Figure 1), and hence it was selected for further formulation development.

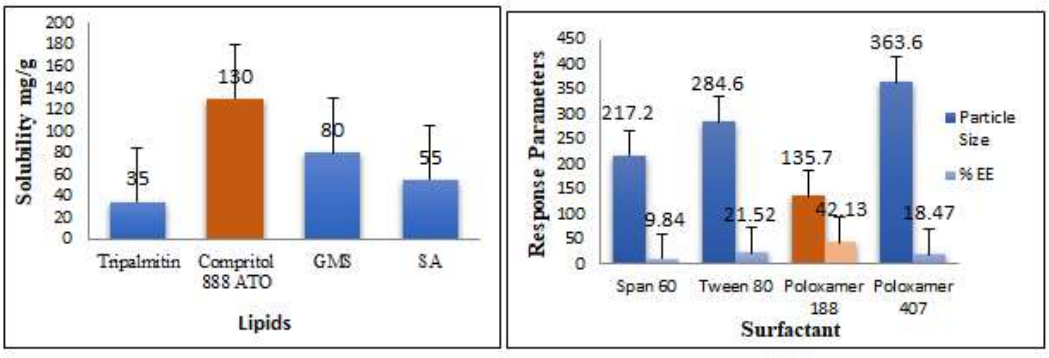

Figure 1: Screening of Lipid and Surfactant (GMS-Glyceryl monostearate, SA- Stearic acid)

Drug-Excipients Compatibility: FTIR spectra of pure Tenofovir and its physical mixture with Compritol® 888 ATO, Poloxamer 188, and soya lecithin are shown in Figure 3. Characteristic Tenofovir peaks corresponding to O–H, C–H, C=O, C=C, C–O, C=S stretching, and C–H bending vibrations were retained in the physical mixture without significant shifts or disappearance, indicating the absence of chemical interaction between Tenofovir and the excipients.

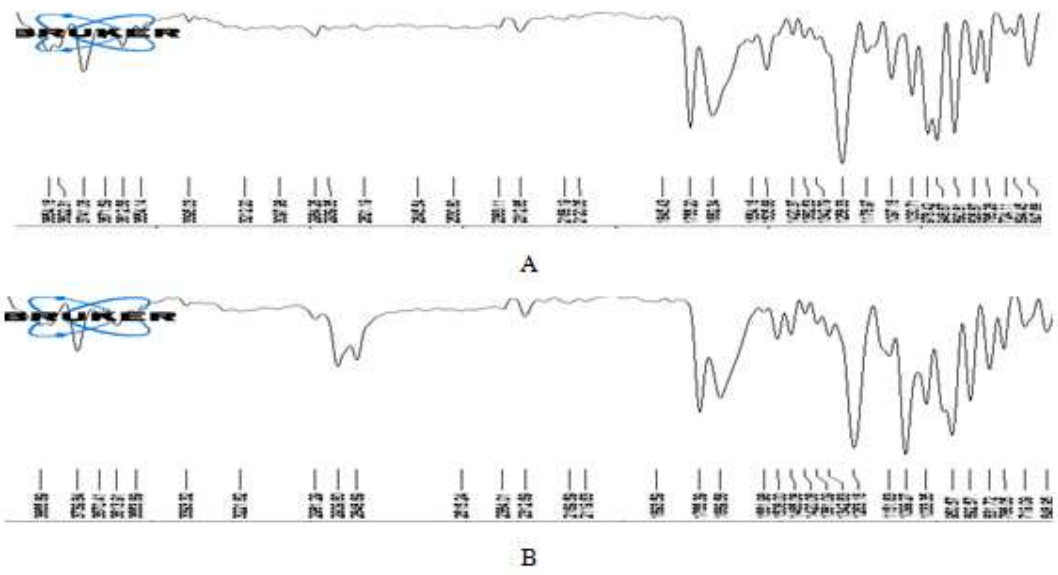

Figure 2: FTIR spectra of A) Tenofovir and B) Physical mixture (Tenofovir + Compritol 888 ATO + Poloxamer 188)

Evaluation of TNF loaded SLNs:

Average Particle Size, Polydispersity Index (PDI), Zeta Potential, and % Entrapment Efficiency (%EE):
Dynamic light scattering analysis revealed that the twelve TNF-loaded SLN formulations exhibited mean particle sizes ranging from 139.4 ± 5.6 to 989.4 ± 24.8 nm with PDI values between 0.26 ± 0.02 and 0.96 ± 0.12 (Table 2). Variations in particle size and distribution were directly influenced by lipid and surfactant concentrations as well as homogenization time. Formulations prepared by the microemulsion technique predominantly produced nanosized particles with acceptable uniformity.

Zeta potential analysis showed values ranging from −9.6 ± 1.2 to −36.9 ± 5.2 mV (Table 4), indicating adequate electrostatic stabilization of the SLNs. Formulations exhibiting zeta potential values greater than ±15 mV were considered physically stable.

Entrapment efficiency values ranged from 27.5 ± 9.8% to 89.3 ± 3.9% (Table 2), with higher lipid content contributing to improved drug entrapment, highlighting the importance of lipid screening in enhancing encapsulation of the hydrophilic drug.

Table 2: Mean Particle size, PDI, Zeta potential and % Entrapment efficiency of TNF loaded SLNs (mean ±SD, n=3)

Formulation Code	Mean Particle Size (nm)	Polydispersity Index (PDI)	Zeta potential (ZP)	% Entrapment Efficiency (%EE)
F1	139.4±23.7	0.54±0.06	-9.6±-1.2	32.3±5.4
F2	315.1±9.3	0.31±0.05	-24.3±-3.6	67.6±4.2
F3	699.7±13.4	0.73±0.13	-32.2±-4.7	89.3±3.9
F4	989.4±24.8	0.94±0.17	-36.9±-5.2	74.5±6.9
F5	523.6±16.3	0.69±0.08	-28.2±-2.6	44.1±2.6
F6	323.5±12.6	0.43±0.07	-23.6±-1.9	58.6±2.6
F7	195.4±8.2	0.26±0.02	-21.7±-1.2	82.7±2.9
F8	412.3±14.7	0.75±0.16	-19.6±-2.4	70.3±3.5
F9	564.8±21.3	0.53±0.04	-22.4±-2.6	64.2±2.9
F10	316.2±10.5	0.39±0.06	-23.7±-1.7	65.8±2.1
F11	472.6±14.2	0.86±0.08	-21.1±-4.6	59.6±4.8
F12	887.8±25.7	0.96±0.12	-19.6±-5.2	27.5±9.8

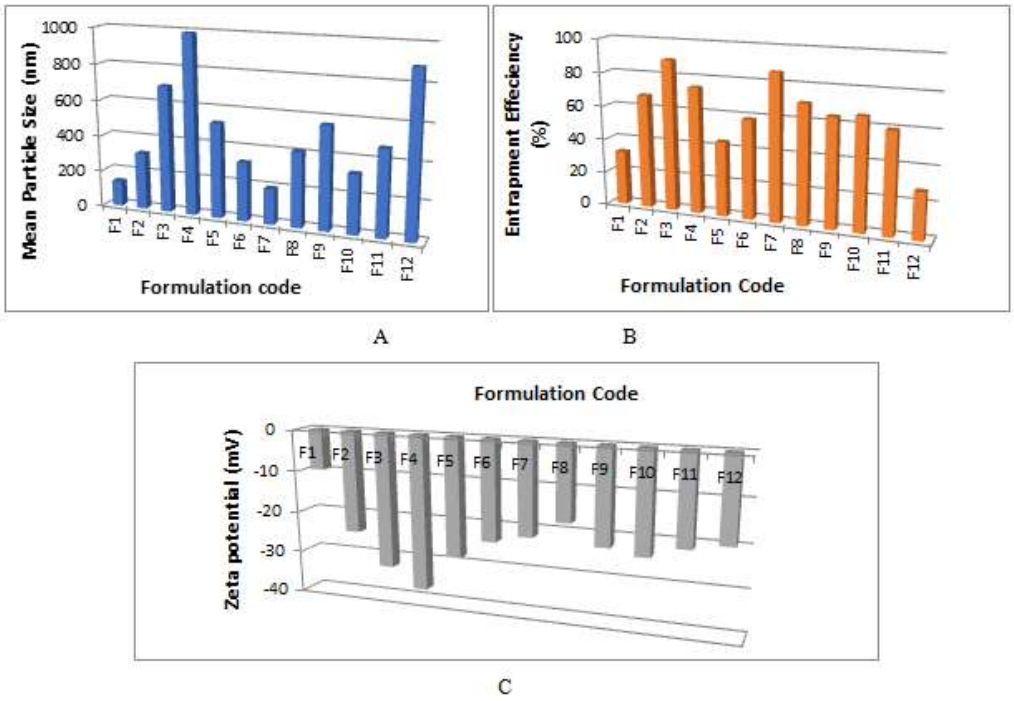

Figure 3: Effect of Formulation Factors (Concentration of Lipid, Surfactant & Homogenization Time) on A) Particle size, B) % Entrapment Efficiency, C) Zeta potential

Factors Affecting TNF-Loaded SLN Formulation

As illustrated in figure 3, particle size, PDI, zeta potential, and entrapment efficiency were all highly impacted by three important formulation variables: lipid concentration, surfactant concentration, and homogenization time

Effect of Lipid Concentration: Increasing lipid content from 2.5 to 10% w/v (F1–F4) led to larger particle sizes (139.4 ± 5.6 to 989.6 ± 23.2 nm) and higher PDI (0.54 ± 0.06 to 0.94 ± 0.17) due to increased dispersion viscosity and interfacial tension causing globule coalescence. Zeta potential became more negative (−9.6 ± 1.2 to −36.9 ± 5.2 mV) reflecting the anionic nature of the lipid. Entrapment efficiency improved with higher lipid content, likely from increased internal volume and faster solidification preventing drug leakage.

Effect of Surfactant Concentration: Varying Poloxamer 188 from 0.5 to 2% w/v (F5–F8) showed that 1.5% w/v was optimal, yielding minimal particle size (195.4 ± 8.2 nm), low PDI (0.26 ± 0.02), and maximum entrapment efficiency (82.7 ± 2.9%). Higher surfactant concentrations produced micelles, increased PDI, and reduced drug encapsulation, while lower concentrations resulted in weaker steric stabilization and smaller negative zeta potential.

Effect of Homogenization Time: Increasing homogenization from 30 to 60 min (F9–F12) reduced particle size (564.8 ± 21.3 to 316.2 ± 10.5 nm) due to enhanced droplet deformation. Prolonged homogenization (>60 min) increased PDI (up to 0.96 ± 0.12) and decreased entrapment efficiency, likely from particle aggregation and drug leakage through the destabilized surfactant layer. Zeta potential remained largely unaffected by homogenization time.

Prolonged homogenization (>60 min) resulted in increased PDI and reduced entrapment efficiency, which can be attributed to over-processing effects. Excessive shear forces may disrupt the surfactant layer at the lipid–aqueous interface, reducing interfacial stability and promoting droplet coalescence, leading to broader particle size distribution. Furthermore, extended homogenization may enhance drug diffusion from the lipid core into the external phase and induce partial lipid matrix rearrangement, thereby decreasing entrapment efficiency.

In-vitro Drug Release Studies: Resulting data from in-vitro drug release studies were fit into cumulative graphs as shown in Figure 4, indicated that SLNs exhibited sustained release of 76–89% over 24 h, whereas pure Tenofovir solution released nearly 100% within 4 h. Most formulations showed an initial burst release of ~40% within 3–4 h, followed by a gradual, sustained release. Kinetic analysis indicated that drug release from SLNs followed first-order kinetics ($R^2 = 0.923$) and an exponent (n) of 0.68 from the Korsmeyer-Peppas model indicated non-Fickian (anomalous) diffusion.

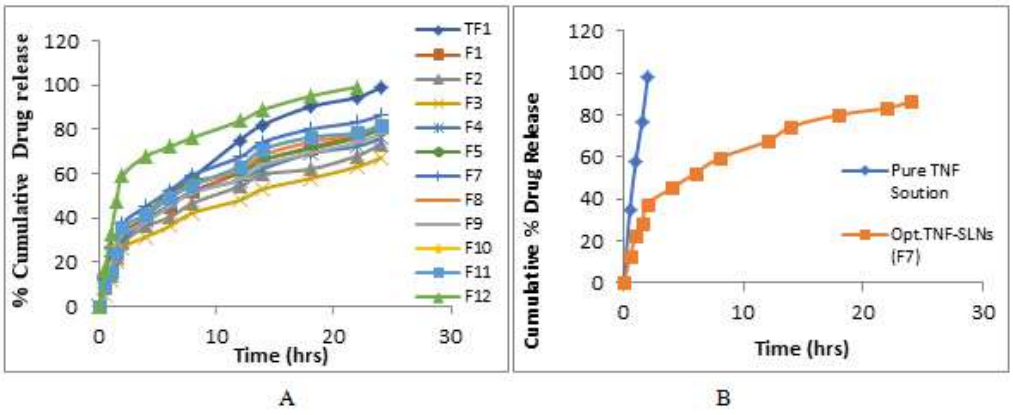

Figure 4: A. TNF-loaded SLN formulations F1–F12's in vitro drug release profile
B. Comparing the Optimized TNF-SLNs (F7) and Pure TNF Solution's in vitro release profiles

CHARACTERIZATION OF OPTIMIZED TNF LOADED SLNS FORMULATION:

Differential scanning Calorimetry (DSC): DSC thermograms of pure Tenofovir, the physical mixture, and optimized SLNs (F7) were displayed in Figure 5A. Pure tenofovir showed a distinct endothermic peak.at 117.05°C while the physical mixture displayed peaks at 72.8 °C (Compritol® 888 ATO) and 117.05 °C (Tenofovir). The optimized SLNs showed only the lipid peak at 72.8 °C, indicating successful entrapment of Tenofovir within the lipid matrix and partial drug amorphization.

Powder X-Ray Diffraction (PXRD): PXRD analysis (Figure 5B) confirmed the crystalline nature of pure Tenofovir, with characteristic peaks at 2θ = 2.6, 9.8, 18.9, 20.2, 23.5, 25.1, and 31.6°. The physical mixture retained these peaks, whereas the optimized SLNs (F7) showed reduced intensity and partial disappearance of these peaks, indicating loss of crystallinity and successful drug incorporation into the lipid matrix.

Scanning Electron Microscopy (SEM): SEM micrographs of the optimized formulation (F7) provided a general indication of particle morphology. SEM micrographs of F7 shown in Figure 5C revealed nearly spherical particles with smooth surfaces in the nanometer range.

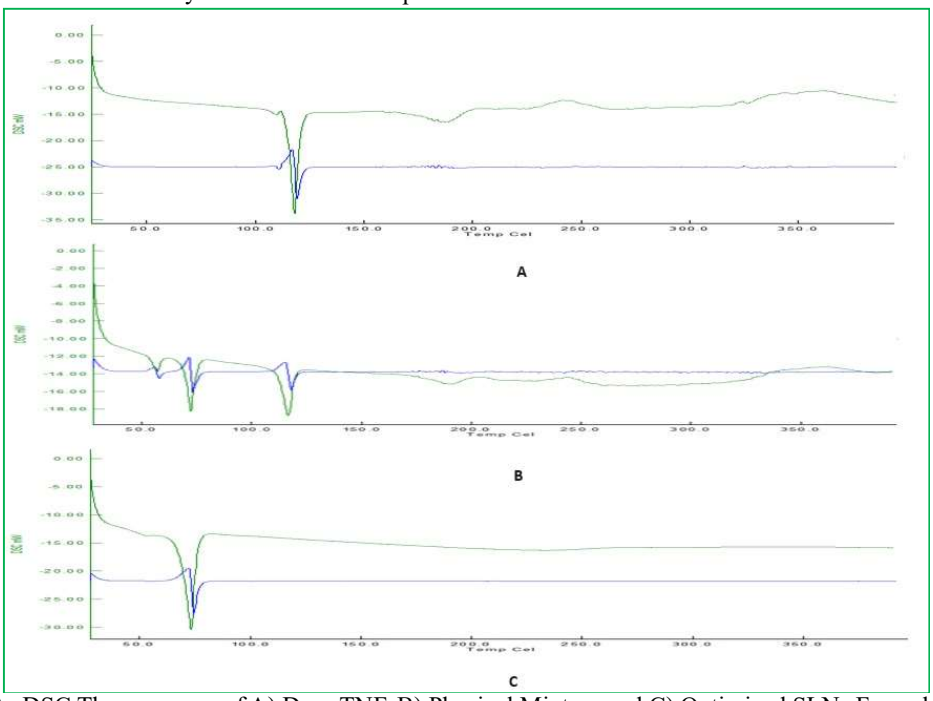

Figure 5A: DSC Thermograms of A) Drug TNF, B) Physical Mixture and C) Optimized SLNs Formulation (F7)

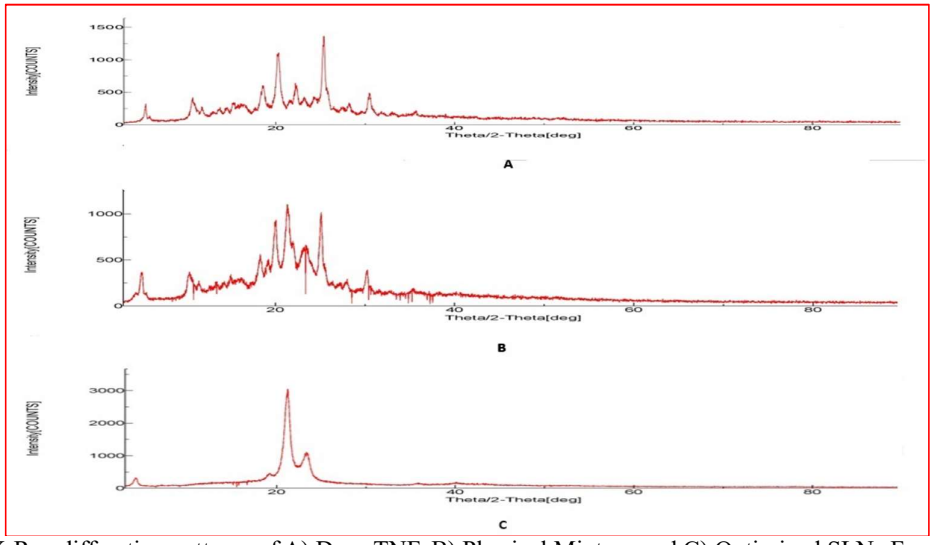

Figure 5B: X-Ray diffraction patterns of A) Drug TNF, B) Physical Mixture and C) Optimized SLNs Formulation (F7)

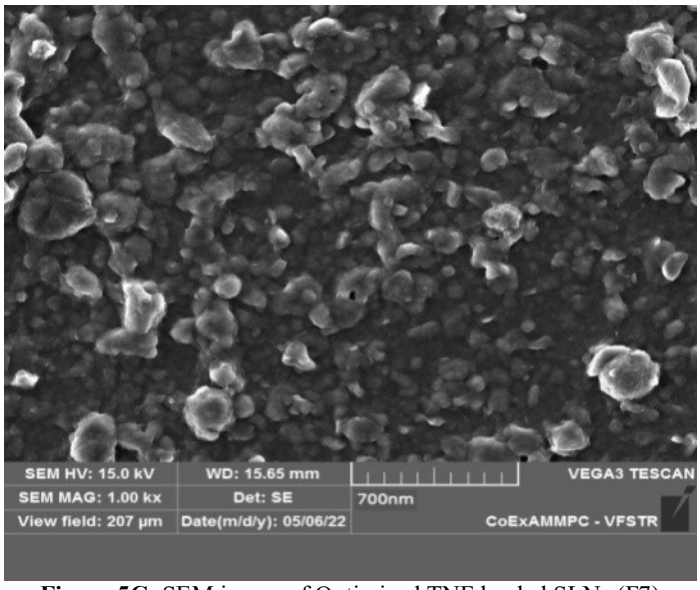

Figure 5C: SEM image of Optimized TNF loaded SLNs (F7)

In-vivo Pharmacokinetic Study: The mean plasma concentration–time profiles of TNF-loaded SLNs and pure Tenofovir solution are shown in Figure 8, and pharmacokinetic parameters are summarized in Table 3. TNF-loaded SLNs achieved a Cmax of 436.32 ± 14.21 ng/mL, compared to 46.52 ± 5.23 ng/mL for the pure drug. The AUC_{0-24} increased from 1026.34 ± 156.23ng h/mL (pure TNF) to 6362.43 ± 82.30 ng h/mL (SLNs), and Tmax was extended from 2 to 4 h. The mean residence time also increased from 17.74 ± 1.68 h to 56.23 ± 3.12 h. Overall, oral administration of TNF-loaded SLNs enhanced relative bioavailability by 7.2-fold ($p < 0.05$), demonstrating significant improvement in TNF pharmacokinetics.

Table 3: Pure TNF solution and optimized TNF-loaded SLNs (F7) pharmacokinetic profile, mean±SD (n=6)

Parameter	Pure TNF Solution	Opt. TNF loaded SLNs(F7)
Cmax (ng/mL)	46.52±5.23	436.32± 14.21
Tmax (hrs)	1.5±0.5	4.5± 0.5
K_a (hrs^{-1})	0.56± 0.19	2.39±0.05
K_E (hrs^{-1})	1.52± 0.39	0.37±0.23
$t_{1/2}$(hrs)	12.6±1.42	28. 41±2.35
AUC_{0-24}(ng/hr/mL)	1026.34± 156.23	6362.43±82.30
$[AUC]_{0-\infty}$(ng/hr/mL)	1249.58±137.56	8983.16±138.26
MRT (hrs)	17.74±1.68	56.23± 2.12

Tissue Distribution: The percentage distribution of Tenofovir in various organs after oral administration of pure TNF and TNF-loaded SLNs (10 mg/kg) is summarized in Table 4. Pure TNF predominantly accumulated in RES organs in the order: liver > spleen > kidney > lungs > pancreas > heart > brain. In contrast, TNF-loaded SLNs showed enhanced brain targeting, with the distribution order: brain > kidney > liver > heart > spleen > lungs > pancreas (Figure 8). These results indicate that SLNs effectively improved CNS delivery while reducing RES uptake compared to the pure drug.

The tissue distribution data represent the relative percentage of drug recovered from selected organs at a single time point (24 h) and are intended for comparative evaluation of organ-specific distribution The markedly higher brain distribution observed with SLNs therefore indicates preferential targeting rather than complete dose recovery.

Table 4: The results of In-vivo Tissue Distribution studies of Pure TNF solution and TNF loaded SLNs (mean± SD, n=6)

Organ	Pure TNF solution (% Drug Distribution)	TNF loaded SLNs dispersion (% Drug Distribution)
Liver	14.16±0. 38%	2.08±0.08
Spleen	12.18±0.12%	1.29±0.02
Lungs	9.23±0.56%	1.13±0.04
Kidney	11.52±0.31%	2.32±0.09
Pancreas	4.29±0.27	1.02±0.06
Heart	2.36±0.14	1.98± 0.19
Brain	0.09±0.02	38.12±0.26

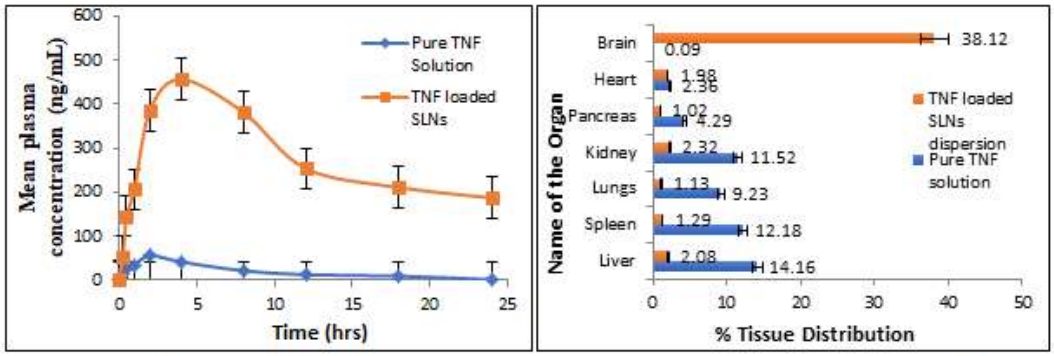

A B

Figure 6: A: Pharmacokinetic Profile and B: Tissue Distribution of TNF after single oral dose of Opt. TNF-SLNs and Pure TNF Solution.

Stability Studies: The optimized TNF-loaded SLNs (F7) were evaluated for stability over six months at 5 ± 3°C/45% RH, 30 ± 2°C/60% RH, and 40°C/75% RH (Table 5). At 5°C and 30°C, there were no discernible changes in particle size, PDI, zeta potential, or entrapment efficiency. At 40°C/75% RH, particle size and PDI increased, and entrapment efficiency decreased, likely due to drug leakage and particle aggregation. Overall, F7 demonstrated good stability under refrigeration and room temperature conditions.

Table 5: Stability study data of optimized TNF loaded SLNs (F7) over 6 months

Storage Condition	Stability Parameter	Sampling Intervals (Days)				
		0	**30**	**60**	**90**	**180**
5±3°c/45%RH	PS (nm)	195.4±8.2	195.4±8.2	195.4±8.2	196.2±6.2	196.2±7.3
	PDI	0.26±0.02	0.26±0.02	0.26±0.02	0.26±0.02	0.27±0.04
	ZP (mV)	-21.7±-1.2	-21.7±-1.2	-21.7±-1.2	-21.7±-1.2	-21.5±-1.1
	EE (%)	86.2±2.9	86.2±2.9	86.3±2.9	86.2±2.9	86.4±3.1
30±2°c/ 60%RH	PS (nm)	195.4±8.2	195.4±8.2	195.4±8.2	197.4±9.1	195.4±9.6
	PDI	0.26±0.02	0.26±0.02	0.26±0.02	0.27±0.04	0.27±0.04
	ZP (mV)	-21.7±-1.2	-21.7±-1.2	-21.7±-1.2	-21.4±-1.1	-21.4±-1.3
	EE (%)	86.2±2.9	86.2±2.9	86.2±1.9	85.9±3.2	85.9±3.4
40°c/75%RH	PS (nm)	195.4±8.2	201.2±8.6	213.4±8.6	226.4±9.1	245.2±13.2
	PDI	0.26±0.02	0.27±0.05	0.27±0.05	0.28±0.06	0.32±0.04
	ZP (mV)	-21.7±-1.2	-21.7±-1.4	-21.6±-1.3	-21.6±-1.3	-20.2±-2.6
	EE (%)	86.2±2.9	85.7±1.8	83.2±1.2	82.2±1.5	81.5±2.4

PS- Particle Size; PDI- Polydispersity Index; ZP- Zeta potential; EE- Entrapment Efficiency

DISCUSSION

The results of this work shed light on how solid lipid nanoparticles (SLNs) can get around Tenofovir's biopharmaceutical restrictions. Tenofovir is a hydrophilic antiviral medication with poor membrane permeability and low oral bioavailability. A key factor in improving medication encapsulation and release behaviour was the thoughtful choice of Compritol® 888 ATO as the lipid matrix. The heterogeneous combination of mono-, di-, and triglycerides found in Compritol® 888 ATO solidifies into a less ordered crystalline lattice. The remarkable entrapment efficiency shown in the improved formulation can be explained by these lattice flaws, which provide internal voids that promote Tenofovir molecular accommodation and decrease drug ejection during lipid recrystallization.

Poloxamer 188 functioned as a functional excipient that affected particle formation and biological performance in addition to acting as a stabilizing surfactant. Its amphiphilic block copolymer structure decreases interfacial tension during emulsification and offers steric hindrance at the nanoparticle surface, avoiding aggregation. Formulations exhibiting zeta potential values in the range of ±15–30 mV were considered physically stable. Although higher zeta potential values (≥ ±30 mV) are typically required for purely electrostatic stabilization, the presence of Poloxamer 188 provides additional steric stabilization by forming a protective hydrophilic layer around the nanoparticles. Therefore, the overall stability of the SLNs can be attributed to a synergistic combination of electrostatic repulsion and steric hindrance. Mechanistically, an ideal surfactant concentration guaranteed full lipid droplet surface covering, but high concentrations encouraged Tenofovir micellization and competitive solubilization in the aqueous phase, which decreased drug entrapment. The significance of surfactant–lipid balance in SLN design is highlighted by these findings.

The effect of processing factors, notably homogenization time, further elucidates the structure–property link of SLNs. Long-term homogenization caused the interfacial surfactant layer to become unstable, which resulted in particle coalescence and increased drug penetration into the external phase. At first, increased shear pressures encouraged droplet breakup and particle size reduction. The observed rise in PDI and decrease in entrapment efficiency at longer homogenization durations are explained by this mechanistic interaction.

Solid-state characterization revealed critical insights into drug disposition within the lipid matrix. The drug's partial amorphization and molecular dispersion are indicated by the diminution of distinctive PXRD peaks and the absence of Tenofovir's melting endotherm in DSC thermograms. Improved dissolving and prolonged release are made possible by amorphization, which lowers lattice energy and increases thermodynamic solubility. Crucially, the preservation of the lipid melting peak indicates that drug inclusion did not affect lipid crystallinity and validates the structural integrity of the SLN matrix.

Two different mechanistic processes are reflected in the biphasic in vitro release profile: regulated diffusion through the solid lipid core after an initial burst release that is thought to be caused by a drug that is either surface-localized or weakly bound. As is typical of solid lipid systems going through slow polymorphic changes, the non-Fickian release kinetics show that drug diffusion and lipid matrix relaxation take place concurrently. For sustained therapeutic medication levels, this release mechanism is very advantageous.

Several synergistic mechanisms can provide a molecular explanation for the in-vivo pharmacokinetic increase seen with TNF-loaded SLNs. The lipidic structure of SLNs enhances intestinal lymphatic transport, therefore avoiding hepatic first-pass metabolism and enhancing systemic availability. Furthermore, nanoscale particles improve paracellular transport by lengthening mucosal contact time and perhaps temporarily changing epithelial tight junctions. In keeping with the in-vitro release pattern, the extended Tmax and mean residence duration further imply delayed release and decreased clearance.

SLN-mediated altered biodistribution is well supported by tissue distribution data. Improved permeability across the blood–brain barrier and partial evasion of RES clearance are suggested by the decreased accumulation in reticuloendothelial organs and increased brain uptake. The significant enhancement in brain accumulation observed with TNF-loaded SLNs can be attributed to multiple synergistic transport mechanisms. The nanoscale particle size (~200 nm) facilitates uptake via Peyer’s patches through M-cells, promoting intestinal lymphatic transport and partial bypass of hepatic first-pass metabolism. In addition, Poloxamer 188 may inhibit efflux transporters such as P-glycoprotein by modulating membrane fluidity and ATPase activity, thereby reducing drug efflux at both intestinal and blood–brain barrier levels.

Furthermore, SLNs can enhance intestinal absorption by increasing mucosal residence time and potentially modulating tight junction integrity, leading to improved paracellular transport. Transcellular uptake via endocytosis may also contribute to enhanced permeability. At the blood–brain barrier, the lipidic nature and nanoscale size of SLNs may facilitate interaction with endothelial membranes, promoting drug transport into the brain. Collectively, these mechanisms act in a complementary manner to significantly enhance CNS delivery of Tenofovir helps in effective management of HIV infections.

Stability experiments, which show that the lipid matrix maintains structural stability in both ambient and refrigerated environments, further support the resilience of the improved formulation. Increased lipid molecule mobility can be mechanistically connected to the instability seen at high temperatures and humidity, leading to matrix relaxation, drug diffusion, and particle

aggregation, underscoring the significance of suitable storage conditions.

The decrease in entrapment efficiency observed under accelerated conditions (40°C/75% RH) may be attributed to thermally induced lipid matrix reorganization and increased molecular mobility, leading to partial drug expulsion. Solid lipid nanoparticles are known to undergo polymorphic transitions toward more stable crystalline forms during storage, which reduces lattice imperfections and expels entrapped drug. Although DSC and PXRD analyses confirmed the amorphous dispersion of Tenofovir in the freshly prepared formulation, these analyses were not performed after long-term stability studies. Therefore, further investigation using time-dependent DSC and PXRD is required to elucidate potential recrystallization or polymorphic transitions during storage.

Collectively, these mechanistic discoveries validate that Tenofovir-loaded SLNs provide a logical and efficient nanocarrier system that may enhance oral bioavailability, regulate release kinetics, improve drug encapsulation, and facilitate targeted brain delivery. Such a modular delivery strategy has great potential to address unresolved issues in long-term HIV care and enhance therapeutic results.

CONCLUSION

Solid lipid nanoparticles (SLNs) loaded with Tenofovir, developed using the microemulsion approach, demonstrated nanoscale particle size, high entrapment efficiency, and sustained drug release over 24 hours. In vivo pharmacokinetic and tissue distribution studies revealed a significant enhancement in systemic bioavailability and brain uptake compared to the pure drug. Importantly, the observed 7.2-fold increase in oral bioavailability suggests the potential for dose reduction and/or decreased dosing frequency, which may improve patient adherence in long-term HIV therapy. Furthermore, enhanced brain delivery may contribute to more effective management of central nervous system viral reservoirs, potentially reducing the progression of HIV-associated neurocognitive disorders. Improved targeting efficiency may also help in minimizing off-target exposure and associated systemic side effects.

Overall, these findings highlight SLNs as a promising oral drug delivery platform for Tenofovir, with potential clinical benefits. However, further clinical studies are required to validate these outcomes in human subjects.

Future Perspectives

Future studies should focus on advanced characterization using high-resolution imaging (FE-SEM/TEM) and time-dependent DSC/PXRD to assess stability-related changes. Application of Design of Experiments (DoE) and biorelevant dissolution media is recommended for improved formulation optimization and in vivo prediction. Further mechanistic studies on lymphatic uptake and efflux modulation, along with compartmental pharmacokinetic modeling, are warranted. Clinical studies are essential to validate the enhanced bioavailability and brain targeting observed with TNF-loaded SLNs.

ACKNOWLEDGEMENTS

The authors sincerely thank Hindu College of Pharmacy, Guntur, for providing essential facilities and technical support.

Ethical Approval

The study protocol was approved by the Institutional Animal Ethics Committee, Hindu College of Pharmacy, Guntur, India (IAEC-HCOP/2022/07), and all procedures adhered to institutional guidelines.

Author Contributions

Conceptualization and supervision: A. Seetha Devi; Methodology: Ch. Sai Navya Sri, G Mugibunnisa and Manuscript Drafting: M. Sri Rekha, Meraj Sulthana Syed. All authors have read and approved the final manuscript.

Funding

This research received no funding from public, commercial, or non-profit organizations.

Conflict of Interest

The authors declare no conflicts of interest.

REFERENCES

1. Mahajan N, Mujtaba MA, Fule R, Thakre S, Akhtar MS, Alavudeen SS, Anwer MK, Aldawsari MF, Mahmood D, Alam MS. Self-Emulsifying Drug Delivery System for Enhanced Oral Delivery of Tenofovir: Formulation, Physicochemical Characterization, and Bioavailability Assessment. ACS Omega. 2024 Feb 3;9(7):8139-8150.
2. Kwakwa H, Bran J, Ruff J, Sharaf S, Seung H, Choe S, Chua JV. Bictegravir/Emtricitabine/Tenofovir Alafenamide in Adults with HIV/HBV Coinfection: An Open-Label, Single-Arm, Safety and Efficacy Switch Study. Viruses. 2025 Mar 31; 17(4):510. doi: 10.3390/v17040510. PMID: 40284953; PMCID: PMC12030933.
3. Anderson PL, Kiser JJ, Gardner EM, Rower JE, Meditz A, Grant RM. Pharmacological considerations for tenofovir and emtricitabine to prevent HIV infection. Journal of Antimicrobial Chemotherapy. 2011; 66(2):240-250.
4. Giacomelli A, Cossu MV, Moschese D, Carrozzo G, Reato S, Sabaini F, Pozza G, Colombo ML, Fusetti C, Ridolfo AL, Gervasoni C, Antinori S, Gori A. Effectiveness and safety of tenofovir alafenamide/emtricitabine/bictegravir as a first-line regimen in people with HIV: A retrospective observational study. IJID Reg. 2025 Mar 6; 15:100622. doi: 10.1016/j.ijregi.2025.100622. PMID: 40176857; PMCID: PMC11964757.
5. Jean-Michel Molina, Jade Ghosn, Lambert Assoumou, Constance Delaugerre, Michèle Algarte-Genin, Gilles Pialoux, Christine Katlama, Laurence Slama, Geoffroy Liegeon, Lydie Beniguel, Michel Ohayon, Hanane Mouhim, Lauriane Goldwirt, Bruno Spire, Bénédicte Loze, Laure Surgers, Juliette Pavie,

Jérémy Lourenco, Mohamed Ben-Mechlia, Soizic Le Mestre, Daniela Rojas-Castro, Dominique Costagliola,

6. Daily and on-demand HIV pre-exposure prophylaxis with emtricitabine and tenofovir disoproxil (ANRS PREVENIR): a prospective observational cohort study, The Lancet HIV, Volume 9, Issue 8, 2022, Pages e554-e562.
7. Natukunda E, Gaur AH, Kosalaraksa P, Hellström E, Strehlau R, Liberty A, Cox S, Leisegang R, Palaparthy R, Crowe S, Vieira V, Kersey K, Rakhmanina N. Pharmacokinetics, safety and efficacy of elvitegravir/cobicistat/emtricitabine/tenofovir alafenamide in children with HIV aged from 2 years and weighing at least 14 kg. J Int AIDS Soc. 2025 Feb;28(2): e26414. doi: 10.1002/jia2.26414. PMID: 39888251; PMCID: PMC11782835.
8. O'Neil MJ, Heckelman PE, Dobbelaar PH, Roman KJ, Kenny CM, Karaffa LS. The Merck Index: An Encyclopedia of Chemicals, Drugs, and Biologicals. 15th ed. Cambridge: Royal Society of Chemistry; 2013.
9. Shailender J, Ravi PR, Saha P, Dalvi A, Myneni S. Tenofovir disoproxil fumarate loaded PLGA nanoparticles for enhanced oral absorption: Effect of experimental variables and in vitro, ex vivo and in vivo evaluation. Colloids Surf B Biointerfaces. 2017 Oct 1; 158:610-619.
10. Anil B. Jindal, Atharva R. Bhide, Sagar Salave, Dhwani Rana, Derajram Benival, Long-acting parenteral drug delivery systems for the treatment of chronic diseases, Advanced Drug Delivery Reviews, Volume 198, 2023,114862.
11. Cobb, D.A., Smith, N., Deodhar, S. *et al.* Transformation of tenofovir into stable ProTide nanocrystals with long-acting pharmacokinetic profiles. *Nat Commun* **12**, 5458 (2021).
12. Vigano A, Bedogni G, Manfredini V, Giacomet V, Cerini C, di Nello F, Penagini F, Caprio C, Zuccotti GV. Long-term renal safety of tenofovir disoproxil fumarate in vertically HIV-infected children, adolescents and young adults. Clinical drug investigation. 2011; 31(6): 407-15.
13. Fotooh Abadi L, Kumar P, Paknikar K, Gajbhiye V, Kulkarni S. Tenofovir-tethered gold nanoparticles as a novel multifunctional long-acting anti-HIV therapy to overcome deficient drug delivery-: an in vivo proof of concept. J Nanobiotechnology. 2023 Jan 19; 21(1):19. doi: 10.1186/s12951-022-01750-w. PMID: 36658575; PMCID: PMC9850711.
14. Naesens L, Bischofberger N, Augustijns P, Annaert P, Van den Mooter G, Arimilli MN, Kim CU, De Clercq E. Antiretroviral efficacy and pharmacokinetics of oral bis (isopropyloxycarbonyloxymethyl) 9-(2-phosphonylmethoxypropyl) adenine in mice. Antimicrobial agents and chemotherapy. 1998; 42(7):1568-73.
15. Wohl DA, Spinner CD, Flamm J, Hare CB, Doblecki-Lewis S, Ruane PJ, Molina JM, Mills A, Brinson C, Ramgopal M, Clarke A, Crofoot G, Martorell C, Carter C, Cox S, Hojilla JC, Shao Y, Das M, Kintu A, Baeten JM, Grant RM, Mounzer K, Mayer K. HIV-1 infection kinetics, drug resistance, and long-term safety of pre-exposure prophylaxis with emtricitabine plus tenofovir alafenamide (DISCOVER): week 144 open-label extension of a randomised, controlled, phase 3 trial. Lancet HIV. 2024 Aug;11(8):e508-e521.
16. HIV-1 infection kinetics, drug resistance, and long-term safety of pre-exposure prophylaxis with emtricitabine plus tenofovir alafenamide (DISCOVER): week 144 open-label extension of a randomised, controlled, phase 3 trial, The Lancet HIV, Volume 11, Issue 8, 2024, Pages e508-e521.
17. Shailender J, RaviPR, Mrinalini S, Avantika D, Keerthi Priya O.Chitosan nanoparticles for the oral delivery of tenofovir disoproxilfumarate: formulation optimization, characterization and ex vivo and in vivo evaluation for uptake mechanism in rats.Drug Dev IndPharm.2018; 44: 1520-5762.
18. Ignacio Pérez-Valero, Diana Corona Mata,et al. Real-world Effectiveness and Safety of Bictegravir/Emtricitabine/Tenofovir Alafenamide in Comparison With Other Regimens in People With Human Immunodeficiency Virus Starting Therapy With AIDS-Defining Conditions: Results From the CoRIS Cohort—The ACTUAS II Study, *Clinical Infectious Diseases*, 2025; ciaf162.
19. Nakmode DD, Singh B, Abdella S, Song Y, Garg S. Long-acting parenteral formulations of hydrophilic drugs, proteins, and peptide therapeutics: mechanisms, challenges, and therapeutic benefits with a focus on technologies. Drug Deliv Transl Res. 2025 Apr;15(4):1156-1180. doi: 10.1007/s13346-024-01747-y. Epub 2024 Dec 11. Erratum in: Drug Deliv Transl Res. 2025 Apr; 15(4):1454. doi: 10.1007/s13346-024-01781-w. PMID: 39661312; PMCID: PMC11870889.
20. Mandal S, Belshan M, Holec AZhou Y, Destache CJ. 2017. An Enhanced Emtricitabine-Loaded Long-Acting Nanoformulation for Prevention or Treatment of HIV Infection. Antimicrob Agents Chemother 61:10.1128/aac.01475-16.
21. Bertrand J, BarrailTran A, Fayette L, Savic R, Goujard C, Teicher E, Barau C, Pruvost A, Taburet A, Mentré F, Verstuyft C, 2023. Pharmacokinetic Model of Tenofovir and Emtricitabine and Their

Intracellular Metabolites in Patients in the ANRS 134-COPHAR 3 Trial Using Dose Records. Antimicrob Agents Chemother 67: e02339-18.

22. Montaner JS, Lima VD, Harrigan PR, Lourenço L, Yip B, Nosyk B, Wood E, Kerr T, Shannon K, Moore D, Hogg RS. Expansion of HAART coverage is associated with sustained decreases in HIV/AIDS morbidity, mortality and HIV transmission: the "HIV Treatment as Prevention" experience in a Canadian setting. PloS one. 2014; 9(2): e87872.
23. Thurman, Andrea R. et al. Safety and Pharmacokinetics of a Tenofovir Alafenamide Fumarate-Emtricitabine based Oral Antiretroviral Regimen for Prevention of HIV Acquisition in Women: A Randomized Controlled Trial. eClinicalMedicine, 2024, Volume 36, 100893.
24. Brar, Indira MDa, Ruane, Peter J. MDb, Berhe, Mezgebe MD, MPHc, Brinson, Cynthia MDd, Benson, Paul Doe, Henry, Keith MDf, Liu, Hui PhDg, Ramgopal, Moti MDh. Efficacy and safety of switch to bictegravir/emtricitabine/tenofovir alafenamide from dolutegravir/abacavir/lamivudine: Results from an open-label extension of a phase 3 randomized, double-blind, multicenter, active-controlled, non-inferiority study. Medicine 104(8): p e41482, February 21, 2025.
25. Mitchell KM, Boily MC, Hanscom B, Moore M, Todd J, Paz-Bailey G, Wejnert C, Liu A, Donnell DJ, Grinsztejn B, Landovitz RJ, Dimitrov DT. Estimating the impact of HIV PrEP regimens containing long-acting injectable cabotegravir or daily oral tenofovir disoproxil fumarate/emtricitabine among men who have sex with men in the United States: a mathematical modelling study for HPTN 083. Lancet Reg Health Am. 2023 Jan 17; 18:100416.
26. Kaul M. HIV's double strike at the brain: neuronal toxicity and compromised neurogenesis. Front Biosci. 2008; 13: 2484–94.
27. Antinori A, Arendt G, Becker JT, Brew BJ, Byrd DA, Cherner M, Clifford DB, Cinque P, Epstein LG, Goodkin K, Gisslen M, Grant I, Heaton RK, Joseph J, Marder K, Marra CM, McArthur JC, Nunn M, Price RW, Pulliam L, Robertson KR, Sacktor N, Valcour V, Wojna VE. Updated research nosology for HIV-associated neurocognitive disorders. Neurology. 2007; 69: 1789-1799.
28. Lavanya V, Sarah AT. The transport of anti-HIV drugs across blood–CNS interfaces: Summary of current knowledge and recommendations for further research. Antiviral Research. 2009; 82 A99–A109.
29. Kavitha SR, Anuja G, Vinod L. Targeting anti-HIV drugs to the CNS. Expert Opin Drug Deliv. 2009; 6(8): 771–784.
30. Mallipeddi R, Rohan LC. Progress in antiretroviral drug delivery using nanotechnology. Int J Nanomed. 2010; 5(1):533–547.
31. Lembo D, Cavalli R. Nanoparticulate delivery systems for antiviral drugs. Antivir Chem Chemother. 2010; 21:53–70.
32. Li X, Tsibouklis J, Weng T. Nano carriers for drug transport across the blood – brain barrier. J Drug Target. 2017; 252330: 17–28.
33. Vyas SP, Khar RK. Targetted and controlled drug delivery, Novel carrier systems. Delhi: CBS publishers and distributers; 2007.
34. Jourghanian P, Ghaffari S, Ardjmand M, Haghighat S, Mohammadnejad M. Sustained release curcumin loaded solid lipid nanoparticles. Adv Pharm Bull. 2016; 6(1):17-21.
35. Muller HR, Mader K, Gohla S. Solid lipid nanoparticles (SLN) for controlled drug delivery- a review of the state of the art. European journal of pharmaceutics and biopharmaceutics. 2000; 50 (1): 161-177.
36. Li H, Zhao X, Ma Y, Zhai G, Li L, Lou H. Enhancement of gastrointestinal absorption of quercetin by solid lipid nanoparticles. J Control Release. 2009; 133: 238-244.
37. Uner M, Yener G. Importance of Solid Lipid Nanoparticles (SLN) in various administration routes and future perspectives. International Journal of Nanomedicine. 2007; 2(3): 289–300.
38. O'Driscoll, Lipid-based formulations for intestinal lymphatic delivery. European Journal of Pharmaceutical Sciences 2002; 1(5): 405–415.
39. Stuchlik M, Zak S. Lipid-based vehicle for oral drug delivery. Biomedical Papers of the Medical Faculty of the University Palacky. 2001; 145(2): 17–26.
40. Wasan KM. 2009. The biological functions of lipid excipients and the implications for pharmaceutical products development. J Pharm Sci 98(2): 379–382.
41. Kasongo W, Jana P, Rainer H M, Roderick B W. Selection and Characterization of Suitable Lipid Excipients for use in the Manufacture of Didanosine-Loaded Solid Lipid Nanoparticles and Nanostructured Lipid Carriers. Journal of pharmaceutical sciences. 2011; 100(12).
42. Shweta G, Rajesh K, Narendra C, Ambikanandan M, Abdelwahab O. Systematic Approach for the Formulation and Optimization of Solid Lipid Nanoparticles of Efavirenz by High Pressure Homogenization Using Design of Experiments for Brain Targeting and Enhanced Bioavailability. BioMed Research International. 2017; Article ID 5984014, 18 pages.

43. Yadav P, Soni G, Irchhaiya R., Mahor A and Alok S.: Development and characterization of solid lipid nanoparticles by solvent diffusion- evaporation method for topical delivery. Int J Pharm Sci Res 2014; 5(3): 1028-34.doi: 10.13040/IJPSR.0975-8232.5(3).1028-34

44. Amanpreet K, Shishu G, Om Prakash K. Thermal analysis and quantitative characterization of compatibility between diflunisal and lipid excipients as raw materials for development of solid lipid nanoparticles. Thermochimica Acta. 2016; 643: 23–32.

45. Song X, Zhao Y, Wu W, Bi Y, Cai Z, Chen Q, Li Y, Hou S. PLGA nanoparticles simultaneously loaded with vincristine sulfate and verapamil hydrochloride: systematic study of particle size and drug entrapment efficiency. International journal of pharmaceutics. 2008; 350(1): 320-9

46. Rao MP, Manjunath K, Bhagawati ST, Thippeswamy BS. Bixin loaded solid lipid nanoparticles for enhanced hepatoprotection–Preparation, characterisation and in vivo evaluation. International journal of pharmaceutics. 2014; 473(1): 485-92.

47. Nguyen T-T-L, Duong V-A. Solid Lipid Nanoparticles. *Encyclopedia*. 2022; 2(2):952-973.

48. Priyanka K, Sathali AA. Preparation and evaluation of montelukast sodium loaded solid lipid nanoparticles. J Young Pharm. 2012 Jul; 4(3): 129-37.

49. Kesharwani R, Sachan A, Singh S, Pate D. Formulation & Evaluation of Solid Lipid Nanoparticle (SLN) Based Topical Gel of Etoricoxib. J App Pharm Sci. 2016; 6 (10): 124-131

50. Viveksarathi K, Krishnamoorthy K. Compatibility studies of rasagiline mesylate with selected excipients for an effective solid lipid nanoparticles formulation. Int J Pharm Pharm Sci. 2015; 7(1): 73-8.

51. Mahajan N, Mujtaba MA, Fule R, Thakre S, Akhtar MS, Alavudeen SS, Anwer MK, Aldawsari MF, Mahmood D, Alam MS. Self-Emulsifying Drug Delivery System for Enhanced Oral Delivery of Tenofovir: Formulation, Physicochemical Characterization, and Bioavailability Assessment. ACS Omega. 2024 Feb 3;9(7):8139-8150.

52. Kandagal PB, Manjunatha DH, Seetharamappa J, Kalanur KK. RP-HPLC Method for the Determination of Tenofovir in Pharmaceutical Formulations and Spiked Human Plasma, Analytical Letters. 2008; 41(4): 561-570.

53. Ghanem HA, Nasr AM, Hassan TH, Elkhoudary MM, Alshaman R, Alattar A, Gad S. Comprehensive Study of Atorvastatin Nanostructured Lipid Carriers through Multivariate Conceptualization and Optimization. *Pharmaceutics*. 2021; 13(2):178.

54. Sanyog J, Meghal A, Mistry N, Swarnakar K. Enhanced dermal delivery of acyclovir using solid lipid nanoparticles. Drug Deliv. And Transl. Res. 2011; 1: 395–406.

55. Pandya NT, Jani P, Vanza J, Tandel H. Solid lipid nanoparticles as an efficient drug delivery system of olmesartan medoxomil for the treatment of hypertension. Colloids Surf B Biointerfaces. 2018 May 1; 165:37-44.

56. Anand KK, Parameswara RV, Priyanka K, Sanjay KS, Sanjay S. Development and Evaluation of Solid Lipid Nanoparticles of Raloxifene Hydrochloride for Enhanced Bioavailability. BioMed Research International. 2013; Article ID 584549, 9 pages.

57. Haniza H, Ramatu OB, Siti KA, Ekram A, Meor MRM, Affandi M, Ahmad FS, Rusliza B. Acyclovir-Loaded Solid Lipid Nanoparticles: Optimization, Characterization and Evaluation of Its Pharmacokinetic Profile. Nanomaterials. 2020; 10, 1785.

58. Su Li, Zhaoshuai Ji, MeiJuan Zou, Xin Nie, Yijie Shi, Gang Cheng. Preparation, Characterization, Pharmacokinetics and Tissue Distribution of Solid Lipid Nanoparticles Loaded with Tetrandrine. AAPS PharmSciTech. 2011; 12(3).

59. Nandini PT, Doijad RC, Shivakumar HN, Dandagi PM, Formulation and evaluation of gemcitabine-loaded solid lipid nanoparticles. Drug Deliv. 2015; 22(5): 647–651.

60. Muhammad S, Mir AK, Waheed SK, Maqsood UR, Waqar A, Shahzeb K. Fabrication, Characterization, and In Vivo Evaluation of Famotidine Loaded Solid Lipid Nanoparticles for Boosting Oral Bioavailability. Journal of Nanomaterials. 2017; Article ID 7357150, 10 pages.